PHYSICAL REVIEW B VOLUME 45, NUMBER 13 1 APRIL 1992-I

Raman scattering from A_g and B_{1g} phonons in $Bi_2Sr_2Ca_{n-1}Cu_nO_{2n+4}$ ($n=1,2$)

Ran Liu and M. V. Klein
Department of Physics and Materials Research Laboratory, University of Illinois at Urbana-Champaign,
1110 W. Green Street, Urbana, Illinois 61801

P. D. Han and D. A. Payne
Department of Materials Science and Engineering and Materials Research Laboratory,
University of Illinois at Urbana-Champaign, 104 South Goodwin Avenue, Urbana, Illinois 61801

(Received 15 July 1991; revised manuscript received 5 November 1991)

Raman measurements were performed on intergrowth-free $Bi_2Sr_2CuO_{6+\delta}$ (2:2:0:1) and $Bi_2Sr_2CaCu_2O_{8+\delta}$ (2:2:1:2) crystals. The phonon spectra of both phases are similar; however, two lowest-frequency phonon lines corresponding to the 28- and 47-cm^{-1} lines in 2:2:1:2 were observed at 20 and 41 cm^{-1} in 2:2:0:1, and, in both cases, these two Raman features appear exclusively in the $z(yy)\bar{z}$ configuration. In addition, two weak A_g lines at 109 and 129 cm^{-1}, which are absent in spectra of 2:2:0:1, were resolved for 2:2:1:2. An overall assignment can be achieved by attributing the two lowest-frequency lines to the first- and second-order scattering features of the amplitude mode of the superstructural modulation, and the other lines to the optical-phonon modes of the distorted orthorhombic subcell. A careful comparison between the spectra of the single- and double-CuO_2-layer Bi compounds enables us to clarify some controversies on assigments of certain phonon modes, especially those in the CuO_2 layer.

I. INTRODUCTION

Although phonons in $Bi_2Sr_2CaCu_2O_{8+\delta}$ have been intensively studied by use of Raman spectroscopy,[1-7] unlike the case of $RBa_2Cu_3O_{7-\delta}$,[8] the assignment of the observed phonon features is still controversial. The main difficulty arises from the existence of complicated local atomic distortions from the symmetry sites of the simple tetragonal unit cell, as well as an incommensurate superstructural modulation,[9-13] which has, so far, not been taken into account in any lattice-dynamical calculation.[14] The factor-group analyses based on *A*2*aa* (Ref. 1) and *Bbmb* (Ref. 4) instead of *I*4/*mmm* did yield reasonable interpretations of the Raman phonon spectra; any possible effect of the superstructural modulation on the lattice vibrational properties was left out of consideration. On the other hand, much less emphasis has been placed on the 2:2:0:1 phase due to its lower T_c and the difficulty of growing samples free of intergrowth of the 2:2:1:2 phase. The work on a ceramic sample[15] as well as a single crystal[1,16] yielded phonon spectra for 2:2:0:1 almost identical to those of 2:2:1:2. However, no experimental data below 50 cm^{-1} and detailed comparisons with spectra of the 2:2:1:2 phase have been reported.

In this work we present *a*-*b*-plane polarized Raman spectra of single crystals of both Bi-based cuprate superconductors in the frequency range of 15–800 cm^{-1}. (No first-order phonon scattering features were observed above 700 cm^{-1}.) Whereas their crystal structures differ from each other mainly by the number of the CuO_2 layers per unit cell and the existence of the Ca separating layer, the other features of the structures, as well as the superstructural modulations, are common to both.[9] Thus, a careful comparison of the phonon spectra of the two materials can provide reliable information on the assignment of the observed phonon lines.

II. EXPERIMENT

Crystals were grown by a flux method using slow cooling in a temperature gradient.[17] The 2:2:0:1 samples were obtained from Cu-rich melts in oxygen atmospheres using a silver crucible and the 2:2:1:2 samples from stoichiometric melts or fluxes containing a small excess of Cu and Ca by using an Al crucible in air. The samples are superconducting with T_c of 9 and 80 K for the 2:2:0:1 and 2:2:1:2 crystals, respectively. No intergrowth between the two phases was found in the x-ray diffraction patterns of the samples used in this work.

Raman spectra were obtained by backscattering from freshly cleaved surfaces with the *c* axis perpendicular to them. The incident light beam of an Ar^+ laser was focused on the sample surfaces mounted in a liquid-helium cryostat to provide power densities of roughly 10 W/cm^2. A double monochromator (Spex model 1401) with a home-made third monochromator as well as smooth sample surfaces enabled us to record the spectra down to 15 cm^{-1}. In this paper we only present spectra excited by the 5145-Å laser line and taken at room temperature, although the low-temperature data will also be discussed.

III. RESULTS AND ANALYSIS

Figure 1 shows the polarized Raman spectra of the 2:2:0:1 and 2:2:1:2 single crystals. A strong *a*-*b* anisotropy in phonon intensities can be clearly seen for both phases. Under the scattering geometry for phonon modes of A_g symmetry 12 and 13 Raman features have

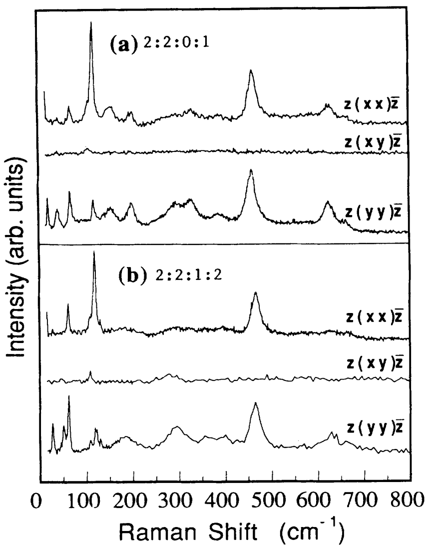

FIG. 1. Raman spectra of the A_g phonon modes in the $z(xx)\bar{z}$ and $z(yy)\bar{z}$ scattering configurations and B_{1g} modes in the $z(xy)\bar{z}$ geometry for a $Bi_2Sr_2CuO_{6+\delta}$ (a) and a $Bi_2Sr_2CaCu_2O_{8+\delta}$ (b) crystals ($l=5145$ Å, $T=293$ K).

been observed, whereas in the spectra of the B_{1g} symmetry one and two phonon lines can be resolved above the noise level, for the 2:2:0:1 and 2:2:1:2 phases, respectively. The fact that the low-frequency phonon lines (Fig. 2) have a one-to-one correspondence, but different frequencies between the spectra of two samples indicate that, as in the case of x-ray diffraction, no intergrowth between the two phases can be detected by Raman spectroscopy for the samples used here.

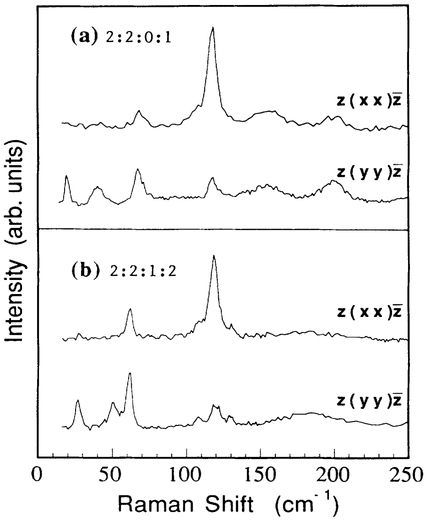

FIG. 2. Low-frequency A_g phonon lines of the $Bi_2Sr_2CuO_{6+\delta}$ (a) and $Bi_2Sr_2CaCu_2O_{8+\delta}$ (b) samples.

The group-theoretical analysis based on the space group $I4/mmm$ of the undistorted body-centered tetragonal structure predicts only $4A_{1g}+0B_{1g}$ and $6A_{1g}+1B_{1g}$ modes under the experimental scattering geometry for the 2:2:0:1 and 2:2:1:2 phases, respectively. The A_{1g} modes in the single-CuO_2-layer material are the symmetric c-axis vibrations of the four sets of the atoms in the BiO and SrO double layers (Bi,Sr,O_{Bi},O_{Sr}). In the double-CuO_2-layer phase the Cu and O atoms in the double plane become Raman active and add another two A_{1g} modes to the other A_{1g} modes identical with those in the 2:2:0:1 phase, and these extra O atoms give rise to a B_{1g} mode (the out-of-phase vibrations) as well.

Since we find many more observed phonon lines than expected from the idealized structure, their assignments require theoretical analysis, which take into account both the local atomic distortion and the superstructural modulation. For a complete consideration the superspace group $N\,Bbmb/11\bar{1}$ (Ref. 10) should be used to describe the one-dimensional incommensurately modulated structure, which, however, will give a huge number of vibrational modes. To simplify the analysis, we neglect the optical phonon modes folded to the Brillouin-zone center by the superstructural modulation. These are usually expected to have weak Raman activities. The effect of such a modulation on the Raman spectra could be approximated merely by introducing some folded acoustic phonon modes or the vibrational modes of the modulation. Therefore, we can assign most of the observed phonon features to the optical vibrational modes of the orthorhombic subcell and the excess low-frequency lines to the modes induced by the superstructural modulation.

Two kinds of space group were proposed to describe the subcell structure, either with centrosymmetry, i.e., *Fmmm*,[11,13] *Bbmb*,[10] or without centrosymmetry, i.e., *A2aa*.[13] Since the infrared spectra[18] show phonon lines with different frequencies from those of Raman spectra, we adopt the centrosymmetric structure *Bbmb* with point group D_{2h} in the present work. The analysis of the phonon modes is straightforward by using the site symmetries given by Imai *et al.*[10] For the purpose of a clarified discussion and of easy comparison either with the theoretical calculation, which was based on the tetragonal structure, or with the work done on other cuprate superconductors, we divide these modes into two categories with respect to the idealized tetragonal structure. The first category contains the zone-center modes and the second the zone-boundary modes, which become Raman active after Brillouin-zone folding along the [110] ([$1\bar{1}0$]) direction of the tetragonal zone due to the orthorhombic distortion. For the orthorhombic structure the A_{1g} modes in the tetragonal structure become A_g modes and the B_{1g} mode retains its symmetry (see Table I). We label the additional modes of these symmetries due to the unit-cell doubling by A_g^* and B_{1g}^*, and the corresponding atomic displacements are shown in Fig. 3. A strong a-b anisotropy in the vibrational pattern for these additional modes will usually be reflected by a large a-b anisotropy in the Raman intensities of the A_g^* modes. In the experimental configuration the orthorhombic subcell will thus give rise to a total of $9A_g+5B_{1g}$ and $12A_g+7B_{1g}$ modes for the 2:2:0:1 and 2:2:1:2 phases, respectively.

In the case of 2:2:0:1 the expected 9 A_g modes can be well related to the nine Raman features observed in the frequency range of 50–650 cm^{-1} of the A_g spectra [labeled by $z(xx)\bar{z}$ and $z(yy)\bar{z}$ in Fig. 1(a)]. In Table I we

TABLE I. Frequencies symmetries and assignments of the observed Raman modes in both $Bi_2Sr_2CuO_{6+\delta}$ and $Bi_2Sr_2CaCu_2O_{8+\delta}$ crystals.

Frequency 2:2:0:1	(cm^{-1}) 2:2:1:2	Symmetry (D_{2h})	Assignment
20	28	A_g^{**}	amplitude mode
41	47	A_g^{**}	second-order scattering of amplitude mode
67	62	A_g^{*}	Bi *a*-axis vibration
106	106	B_{1g}^{*}	Bi *b*-axis vibration
	109	A_g^{*}	Cu *a*-axis vibration
120	119	A_g	Bi *c*-axis vibration
	129	A_g	Cu *c*-axis vibration
155	180	A_g^{*}	Sr *a*-axis vibration
200	180	A_g	Sr *c*-axis vibration
	285	B_{1g}	O_{Cu} *c*-axis vibration (out-of-phase)
290	295	A_g^{*}	O_{Bi} *a*-axis vibration
325	355	A_g^{*}	O_{Cu} *a*-axis vibration
	not seen	A_g	O_{Cu} *c*-axis vibration (in-phase)
386	400	A_g^{*}	O_{Sr} *a*-axis vibration
459	465	A_g	O_{Sr} *c*-axis vibration
625	630	A_g	O_{Bi} *a*-axis vibration
660	660	A_g^{***}	O_{extra} or folded O_{Bi} *c*-axis vibration

*The Raman modes induced by orthorhombic distortion.

**The Raman modes induced by superstructural modulation.

***The Raman modes induced by extra oxygen atoms (or folded optical modes).

list the tentative assignments for these phonon lines. The peaks at 62 and 119 cm^{-1} can be, respectively, attributed to the A_g and A_g^* vibrations of the Bi atoms. The A_g^* vibration along the *a* axis suggests a stronger *xx* Raman intensity than the *yy* one. The 119-cm^{-1} line, which appears also in 2:2:1:2 at almost the same frequency has been often attributed to the A_g mode of Sr.[4,6,7] Our present assignment of this line is based on comparisons of its frequency with those of the Ba mode in $Tl_2Ba_2CuO_6$ and the Sr mode in $Pb_2Sr_2Ca_{1-x}Y_xCu_3O_8$. The A_g mode of Ba in the isostructural Tl 2:2:0:1 appears at 122 cm^{-1}.[19] The corresponding mode of lighter Sr atoms in Bi 2:2:0:1 is expected to vibrate roughly with a frequency $\omega_{Sr}=\sqrt{M_{Ba}/M_{Sr}}\omega_{Ba}=153$ cm^{-1}, which is higher, instead of lower, than the frequency of Ba mode. Indeed, no Raman features between 100 and 150 cm^{-1} were observed and thus no assignment can be made for the similar Sr mode in $Pb_2Sr_2Ca_{1-x}Y_xCu_3O_8$ in this range.[20] Upon doping Pb into Bi 2:2:1:2, Sapriel *et al.*[7] found that the lines at 61 and 118 cm^{-1} shift downwards by 0.5 and 9.5 cm^{-1}, respectively. They explain the latter frequency change as a decrease in frequency of the Sr mode due to possible replacement of Sr by a portion of Pb atoms. In our opinion, this frequency decrease can more likely be caused by the softening of the Bi mode by the substitution of Pb^{2+} for Bi^{3+}. The two broad phonon lines at 155 and 200 cm^{-1} might correspond to the two similar modes of the Sr atoms. From the fact that the O-Sr-O bond length in the SrO plane is larger than that along the *c* axis[9] we predict that the A_g^* mode would have a lower frequency than the A_g mode. The similar modes of the Sr atoms in $Pb_2Sr_2Ca_{1-x}Y_xCu_3O_8$ were observed at 180 and 240 cm^{-1}.[20]

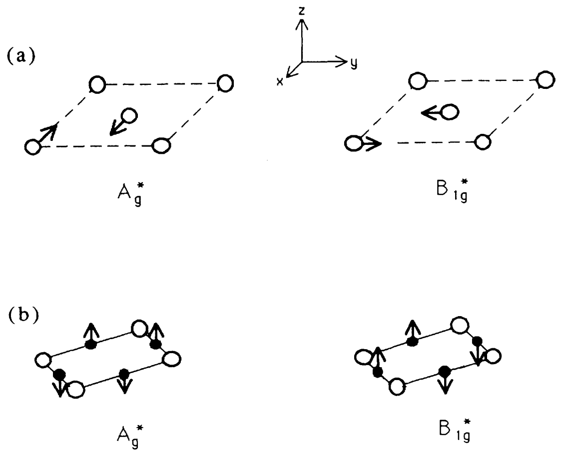

FIG. 3. the vibration patterns of additional modes of A_g and B_{1g} symmetry of the general sites of Bi, Sr, O_{Bi}, and O_{Sr} (and also Cu for 2:2:1:2) atoms (a) and of the O_{Cu} atoms for 2:2:0:1 (b) in the orthorhombic subcell.

The higher-freqeuncy phonon lines should be attributed to the oxygen vibrations. We interpret the Raman features at 290 and 325 cm^{-1} to be the A_g^* modes of the O_{Bi} and O_{Cu} atoms, respectively. The peak around 386 cm^{-1} could come from the O_{Sr} A_g^* mode. Although the theoretically calculated frequency order for the similar in-plane (along *x* or *y*) vibrations[14] favors these interpretations, it is by no means a direct proof, since the calculation was done on the undistorted structure. However, the experimental facts are consistent with our assignment. Figure 1 shows that the 290-cm^{-1} line is the strongest among the three A_g^* features, and its frequency remains almost unchanged upon doubling the $\mathrm{CuO_2}$ layer, whereas the 325- and 386-cm^{-1} lines shift, respectively, by 30 and 14 cm^{-1}. The A_g^* mode with the largest Raman activity should be related to the O mode in the most distorted BiO layers, and its frequency change, due to doubling the $\mathrm{CuO_2}$ layer, is expected to be small because of the large distance between the BiO and the $\mathrm{CuO_2}$ layer in the unit cell. The A_g^* mode of $\mathrm{O_{Cu}}$, on the contrary, should be weakly Raman active, and its frequency is most sensitive to the $\mathrm{CuO_2}$-layer doubling. We identify the strong peaks at 460 and 625 cm^{-1} with the A_g modes of the $\mathrm{O_{Sr}}$ and $\mathrm{O_{Bi}}$ atoms. These assignments have been generally accepted not only because they agree well with theoretical calculations, but also because the similar Raman modes appear at 497 and 599 cm^{-1} for $\mathrm{Tl_2Ba_2CaCu_2O_8}$ (Ref. 19) as well as at 480 and 570 cm^{-1} for $\mathrm{Pb_2Sr_2Ca_{1-x}Y_xCu_3O_8}$ (Ref. 20), whereas the higher-frequency line disappears for $\mathrm{TlBa_2CaCu_2O_7}$ (Ref. 19), which has only one TlO layer per unit cell.[9] However, the 463-cm^{-1} line was recently identified with the A_g mode of $\mathrm{O_{Cu}}$ by Boekholt *et al.*[6] based on its softening below T_c as well as its resonant behavior. Our present observation that this phonon line appears in both 2:2:0:1 and 2:2:1:2 intergrowth-free single crystals with almost the same frequency and intensity indicates undoubtedly that this line should not be attributed to the vibrations in the $\mathrm{CuO_2}$ layer, at least not to a considerable extent.

Up to this point we have assigned all the 9 A_g modes of the subcell. The extra feature at 660 cm^{-1} might result from two possibilities. The first is some vibration of the possibly extra oxygen atoms with formula concentration δ. This assignment can find support from the Raman study of the $\mathrm{Bi_2Sr_2Ca_{1-x}Y_xCu_2O_{8+\delta}}$,[4] where the intensity of this peak increases with x and presumably δ. The second possibility is a folded optical phonon mode. The Raman spectra of $\mathrm{Bi_{2-x}Pb_xSr_2CaCu_2O_{8-y/2}}$ show that the 660-cm^{-1} line is weakened upon the substitution of $\mathrm{Pb^{2+}}$ for the $\mathrm{Bi^{3+}}$, which can strongly suppress the superstructural modulation. In the B_{1g} geometry only one of the five predicted modes can be unambiguously observed at 106 cm^{-1} [Figs. 1(a) and 2(a)]. We attribute this line tentatively to the B_{1g}^* mode of the Bi atoms because of the large atomic distortions in the BiO layers.

In the 2:2:1:2 phase three more A_g phonon lines are expected in comparison with the case of 2:2:0:1. They are the c-axis vibrations of the Cu and O atoms in the double $\mathrm{CuO_2}$ plane and the a-axis vibration of the Cu atoms. These Raman lines are, however, usually very weak for the cuprate superconductors with the double $\mathrm{CuO_2}$ layer separated by a Ca atom.[20] In the present work we can only identify the c axis A_g mode and the a-axis A_g^* mode of the Cu atoms with the weak Raman feature at 129 and 110 cm^{-1}, respectively, which are absent in the spectrum of the 2:2:0:1 phase. The frequencies corresponding to the 129 cm^{-1} phonon mode were identified at 141 and 150 cm^{-1} in $\mathrm{Bi_2Sr_2Ca_{1-x}Y_xCu_2O_{8+\delta}}$ (Ref. 4) and $\mathrm{YBa_2Cu_3O_{7-\delta}}$ (Ref. 8). Another noticeable difference is that the two Sr A_g phonon lines are 152 and 200 cm^{-1} for the 2:2:0:1 phase get closer and become one broad peak with a maximum at 180 cm^{-1} for the 2:2:1:2 sample. A possible reason for this change is that the two A_g vibrational modes might have similar frequencies as seen in the case of 2:2:1:2, and a presumed coupling between the two modes in 2:2:0:1 could split their frequencies. A remarkable frequency shift of the $\mathrm{O_{Cu}}$ A_g^* mode from 325 cm^{-1} in 2:2:0:1 to 355 cm^{-1} shows a hardening of this mode upon the doubling of the $\mathrm{CuO_2}$ layer. A 5-cm^{-1} frequency difference of the Bi A_g^* vibration can also be observed between the spectra of these two phases. The lower frequency of the phonon line in 2:2:1:2 can be related to the increase in the BiO bond length compared with that in 2:2:0:1.[9] All other A_g phonon lines between 50 and 700 cm^{-1} bear a great similarity, both in frequency and in intensity, which suggests that they have small amplitudes on $\mathrm{CuO_2}$ planes, as discussed earlier. Besides the Raman line at 106 cm^{-1}, the same frequency as the B_{1g}^* phonon line in 2:2:0:1, another phonon line of B_{1g} symmetry appears around 285 cm^{-1}. This line, similar to the famous 340-cm^{-1} line in $\mathrm{YBa_2Cu_3O_{7-\delta}}$, has already been definitely assigned to the B_{1g} mode of the O atoms in the double $\mathrm{CuO_2}$ layer.[1]

The remaining two low-frequency lines in the A_g spectra of both phases should be related to some Raman modes induced by superstructural modulation (labeled with A_g^{**} in Table I), since we have exhausted all the A_g modes of the orthorhombic subcell. A strong experimental evidence for such a consideration is the fact that these two lines appear exclusively for the polarizations of both incident and scattered light along the modulation direction, the b axis. Such a strong anisotropy has not yet been reported, although these two lines were observed in some early work for 2:2:1:2.[2,3] Additional experimental evidence can be found in a microscopic Raman investigation on tiny $\mathrm{Bi_{2-x}Pb_xSr_2CaCu_2O_y}$ crystals by Farrow *et al.*,[5] which showed that the phonon lines below 50 cm^{-1} in their spectra in a likely $x(zz)\bar{x}$ configuration disappear at a certain level of Pb doping where the superstructural modulation is strongly suppressed. A possible assignment of the two lines is to the folded acoustic modes due to the superstructural modulation. If we, however, take the incommensurate periodicity $4.7b$ (Ref. 9) and the sound velocity of 4600 m/s for 2:2:1:2 from the data of a Brillouin scattering experiment,[21] the first folded mode is expected at 38 cm^{-1}, which is just between the two observed frequencies. This large discrepancy excludes the possibility of the assignment of the two phonon lines to the folded acoustic modes. Therefore, we tentatively ascribe the lower-frequency line as the amplitude vibrational mode of the superstructure and the second line with a nearly doubled frequency to the second-order scattering of this mode.

IV. CONCLUSIONS

We observed two low-frequency Raman features at 20 and 41 cm^{-1} and 2:2:0:1, which have one-to-one correspondences with the 28 and 47 cm^{-1} lines in 2:2:1:2. The exclusive appearances of these two lines for the light polarizations both along the superstructural modulation in both cases as well as their frequencies suggest that they originate from this modulation and are more likely due to the first- and second-order scattering from the amplitude mode than due to those from the folded acoustic modes. In the high-frequency range ($\omega > 50\ \mathrm{cm}^{-1}$) two additional weak A_g lines, besides the well-known B_{1g} line at 285 cm^{-1}, appear only in the spectra of 2:2:1:2, and can also be related to certain modes in the CuO_2 plane. We have shown that a detailed comparison between the Raman spectra of the Bi-based cuprate superconductors with single and double CuO_2 layer can resolve some discrepancies in the assignment of the Raman-active vibrations of the CuO_2 plane.

ACKNOWLEDGMENTS

One of us (R.L.) thanks F. Slakey and D. Reznik for the technical help. This work was supported through the Science and Technology Center for Superconductivity under NSF Grant No. DMR 8809854.

---

[1] M. Cardona, C. Thomsen, R. Liu, H. G. von Schnering, M. Hartweg, Y. F. Yan, and Z. X. Zhao, Solid State Commun. **66**, 1225 (1988).

[2] F. Slakey, M. V. Klein, E. D. Bukowski, and D. M. Ginsberg, Phys. Rev. B **41**, 2109 (1990).

[3] J. Sapriel, L. Pierre, D. Morin, J. C. Tolenado, J. Schneck, H. Savary, J. Chavignon, J. Primot, C. Daguet, and J. Etrillard, Phys. Rev. B **39**, 339 (1989).

[4] S. Sugai and M. Sato, Jpn. J. Appl. Phys. **28**, L1361 (1989).

[5] L. A. Farrow, R. Ramesh, J.-M. Tarascon, and S. M. Green, in *Raman and Luminescence Spectroscopies in Technology II*, edited by F. Adar and J. E. Griffiths [Proc. SPIE **1336**, 118 (1990)].

[6] M. Boekholt, A. Erle, P. C. Splittberger-Hunnekes, and G. Güntherodt, Solid State Commun. **74**, 1107 (1990); M. Boekholt and G. Güntherodt, Physica C **181**, 179 (1991).

[7] J. Sapriel, J. Schneck, J. F. Scott, J. C. Tolénado, L. Pierre, J. Chavigon, C. Daguet, J. P. Chaminade, and H. Boyer, Phys. Rev. B **43**, 6259 (1991).

[8] See, for example, R. Liu, C. Thomsen, W. Kress, M. Cardona, B. Gegenheimer, F. W. de Wette, J. Prade, A. D. Kulkarni, and U. Schröder, Phys. Rev. B **37**, 7971 (1988).

[9] R. M. Hazen, in *Physical Properties of High Temperature Superconductors II*, edited by D. M. Ginsberg (World Scientific, Singapore, 1990), p. 121.

[10] K. Imai, I. Nakai, T. Kawashima, S. Sueno, and A. Ono, Jpn. J. Appl. Phys. **27**, L1661 (1988).

[11] S. A. Sunshine, T. Siegrist, L. F. Schneemeyer, D. W. Murphy, R. J. Cava, B. Batlogg, R. B. van Dover, R. M. Fleming, S. H. Clarum, S. Nakahara, R. Farrow, J. J. Krajewski, S. M. Zahurak, J. V. Waszczak, J. H. Marshall, P. Marsh, L. W. Rupp, Jr., and W. F. Peck, Phys. Rev. B **38**, 893 (1988).

[12] C. H. Chen, in *Physical Properties of High Temperature Superconductors II* (Ref. 9), p. 199.

[13] P. Bordet, J. J. Capponi, C. Chaillout, J. Schenavas, A. W. Hewat, E. A. Hewat, J. L. Hodeau, M. Marezio, J. L. Tholence, and D. Tranqui, Physica C **156**, 189 (1988).

[14] See, for example, J. Prade, A. D. Kulkarni, F. W. de Wette, U. Schröder, and W. Kress, Phys. Rev. B **39**, 2771 (1989).

[15] V. Popvic, C. Thomsen, M. Cardona, R. Liu, G. Stanisic, R. Kremer, and W. Konig, Solid State Commun. **66**, 965 (1988).

[16] L. A. Farrow, R. Ramesh, and J.-M. Terascon, Phys. Rev. B **43**, 418 (1991).

[17] P. D. Han and D. A. Payne, J. Crystal Growth **104**, 201 (1990).

[18] K. Kamarás, S. L. Herr, C. D. Porter, D. B. Tanner, S. Etemad, and J.-M. Tarascon, Phys. Rev. B **43**, 11 381 (1991).

[19] V. B. Timofeev, A. A. Maksimov, O. V. Misochko, and I. I. Tartakoviskii, Physica C **162-164**, 1409 (1989).

[20] Ran Liu, M. Cardona, B. Gegenheimer, E. T. Heyen, and C. Thomsen, Phys. Rev. B **40**, 1654 (1989).

[21] P. Baumgart, S. Blumenröder, A. Erle, B. Hillebrands, P. Slittgerber, G. Güntherodt, and H. Schmidt, Physica C **162-164**, 1073 (1989).